FOUNDRY / ЛИТЕЙНОЕ ПРОИЗВОДСТВО

UDC 621.74.045 : 53.09
https://doi.org/10.17073/0021-3438-2023-3-54-66

Research article
Научная статья

Porous wax patterns for high-precision investment casting

S.G. Zhilin, N.A. Bogdanova, O.N. Komarov

Institute of Machinery and Metallurgy of Far-Eastern Branch of the Russian Academy of Sciences
681005, Russia, Khabarovsk region, Komsomolsk-on-Amur, Metallurgists str., 1

✉ Sergey G. Zhilin (sergeyzhilin1@rambler.ru)

Annotation: Aerospace, manufacturing, and shipbuilding industries strive to enhance their competitiveness by optimizing material utilization and improving production processes. The investment casting process offers the capability to fabricate intricate and precise components using a diverse range of alloys. However, this method is not without its drawbacks, including high manufacturing costs and a significant rate of defective castings, which can reach up to 30 %. These defects primarily arise from the stresses imposed on the wax patterns and ceramic molds,leading to their distortion. To address this issue, efforts have been made to reduce stress by employing compacted wax powders for the production of investment patterns. However, stress relaxation in the wax patterns remains a concern as it can result in elastic deformation of the compacted material and subsequent alterations in the final product dimensions. To mitigate this issue, a series of tests were conducted with the objective of studying stress relaxation under constant compression strain, as described by the Kohlrausch equation. The obtained results provide valuable insights that enable the prediction of the ultimate dimensions of patterns created using different grades of wax.

Keywords: testing, manufacturing process, investment casting, stress-strain state, compaction, porosity, elastic deformation.

Acknowledgments: This study has received financial support from the Khabarovsk Federal Research Center, Far East Branch, Russian Academy of Sciences. The authors acknowledge the utilization of the Research Data Processing and Storage Center, Far East Branch, Russian Academy of Science, which is funded by the Russian government through the Ministry of Science and Higher Education under Project No. 075-15-2021-663.

For citation: Zhilin S.G., Bogdanova N.A., Komarov O.N. Porous wax patterns for high-precision investment casting. *Izvestiya. Non-Ferrous Metallurgy.* 2023;29(3):54–66. https://doi.org/10.17073/0021-3438-2023-3-54-66

Исследование процессов формирования пористых выплавляемых моделей, применяемых для изготовления высокоточного литья

С.Г. Жилин, Н.А. Богданова, О.Н. Комаров

Институт машиноведения и металлургии Дальневосточного отделения Российской академии наук
681005, Россия, Хабаровский край, г. Комсомольск-на-Амуре, ул. Металлургов, 1

✉ Сергей Геннадьевич Жилин (sergeyzhilin1@rambler.ru)

Аннотация: Конкурентоспособность современных предприятий машино-, судо- и авиастроения во многом определяется материало- и энергоэффективностью технологий, направленных на получение конструкций и узлов деталей ответственного назначения. Применение литья по выплавляемым моделям (ЛВМ) обеспечивает получение заготовок повышенной

размерной и геометрической точности, сложной пространственной конфигурации из широкой номенклатуры сплавов. К недостаткам ЛВМ следует отнести многостадийность процесса и высокую стоимость конечного продукта, что предполагает недопустимость брака, доля которого может достигать 30 %. Брак в ЛВМ преимущественно вызван теплофизическими явлениями, сопровождающими ряд технологических операций и обусловливающими наличие напряжений в структуре воскообразных и керамических материалов, что определяет деформационные процессы в выплавляемых моделях и оболочковых формах. Для устранения негативного влияния теплофизического фактора и снижения напряжений в структурах промежуточных изделий процесса, выплавляемые модели формируют прессованием порошков воскообразных модельных композиций. При этом нерешенным остается вопрос релаксации напряжений в прессовках, приводящих к упругому отклику уплотненного материала и, как следствие, изменению размеров получаемого изделия. Поиск вариантов наиболее рационального режима формирования прессовки привел к необходимости проведения серии экспериментов, в результате которых предполагается достижение релаксации напряжений σ в условиях постоянной деформации сжатия, описываемого уравнением Кольрауша. Полученные в ходе эксперимента результаты позволят прогнозировать конечные размеры прессовок и сформировать математическую модель процесса, актуальную для широкой номенклатуры воскообразных модельных материалов, применяемых в ЛВМ.

Ключевые слова: экспериментальное моделирование, машиностроительные процессы, литье по выплавляемым моделям, напряженно-деформированное состояние, прессовка, пористость, упругий отклик.

Благодарности: Работа выполнена в рамках государственного финансирования Хабаровского федерального исследовательского центра ДВО РАН. Исследования проведены с использованием ресурсов ЦКПН «Центр обработки и хранения научных данных ДВО РАН», финансируемого Российской Федерацией в лице Министерства науки и высшего образования Российской Федерации по проекту № 075-15-2021-663.

Для цитирования: Жилин С.Г., Богданова Н.А., Комаров О.Н. Исследование процессов формирования пористых выплавляемых моделей, применяемых для изготовления высокоточного литья. *Известия вузов. Цветная металлургия*. 2023;29(3):54–66. https://doi.org/10.17073/0021-3438-2023-3-54-66

Introduction

Various industries, including manufacturing, aerospace, and shipbuilding, strive to maintain their competitiveness by reducing production costs while ensuring product quality. Renowned marine engine manufacturers (Wärtsila, Caterpillar, Volvo Penta, MTU, Cummins, etc.) achieve cost reduction through the implementation of reuse and circular processes [1], thereby ensuring long-term competitiveness. The introduction of advanced technologies and innovative manufacturing equipment may result in a significant increase in the final product cost [2]. One approach to cost control during the initial stages of manufacturing, is the use of workpiece casting. For parts subjected to cyclic mechanical and thermal loads, castings should possess high structural strength [3] or hardness [4]. Special requirements also apply to titanium alloy castings and castings for offshore drilling equipment, particularly when centrifugal casting is employed [5], or high dimensional and geometric accuracy is expected.

In shipbuilding, ship propellers represent the largest castings and are typically manufactured using eutectic and near-eutectic high-entropy alloys. These alloys offer high strength and ductility, making them suitable for various operating temperatures [6]. Researchers worldwide are dedicated to enhancing casting quality, improving final product outcomes, and developing new casting repair technologies [7—9].

Simulation plays a crucial role in achieving high-precision casting and reducing defects, as well as operating costs. For example, simulation tools (FEM, volume difference method; vector element or vector gradient methods, etc.) can model the shrinkage that occurs in sandy clay mold casting. The extent of shrinkage is influenced by numerous thermophysical properties of the alloy [10; 11]. It is important to verify the simulation results through physical testing, as most casting simulation tools rely on certain approximate assumptions.

While several codes are available for analyzing conventional sand and clay mold casting processes (e.g., casting of ship propellers and other large ship components), only a limited number of tools can effectively simulate special casting processes such as centrifugal casting, injection molding, or investment casting [12]. Investment casting, in particular, presents significant

challenging for analysis due to the multitude of factors that affect casting quality.

The investment casting process is a multi-stage procedure designed for manufacturing large, solid, complex-shaped parts. In some cases, additional machining processes are not required [13]. With the investment casting process, castings up to 500 mm in size can be produced with a wall thickness of up to 1 mm and a surface roughness of up to R_a = 1.25 μm. The ISO tolerance grade of the casting typically ranges from 11 to 16, provided that the mold tolerances do not exceed grade 8 or 9.

The standard process for investment casting typically involves the following steps:

— manufacturing and assembly of wax patterns;

— layer-by-layer formation of a ceramic shell around the patterns;

— heating and removal of the wax from the mold;

— baking the mold and filling it with molten metal;

— machining of the final cast part.

During the investment casting process, there is a volume variation in the part due to shrinkage or thermal expansion, which can reach 10—14 %. To determine the necessary machining allowances for the casting, it is essential to consider the thermophysical processes involved in metal heating and cooling [14; 15]. These processes can potentially result in manufacturing defects. Investment casting is known for its relatively high defect rate, which can be as high as 30 % [16; 17]. Several negative factors contribute to these defects, including:

— changes in the temperature of wax pattern, leading to surface delamination, shrinkage, or buckling once it is placed into the mold;

— ingress of melted wax into the ceramic mold material during the wax removal process, causing mold destruction during the baking or filling stages.

Figure 1 illustrates a flowchart depicting the occurrence of defects in investment casting. The flowchart includes the following stages:

1 — wax shrinkage, resulting in distortion of the casting geometry:

2 — cracks in the ceramic mold layers caused by the thermal expansion of the wax during heating and removal;

3 — wax expansion in the ceramic shell pores during

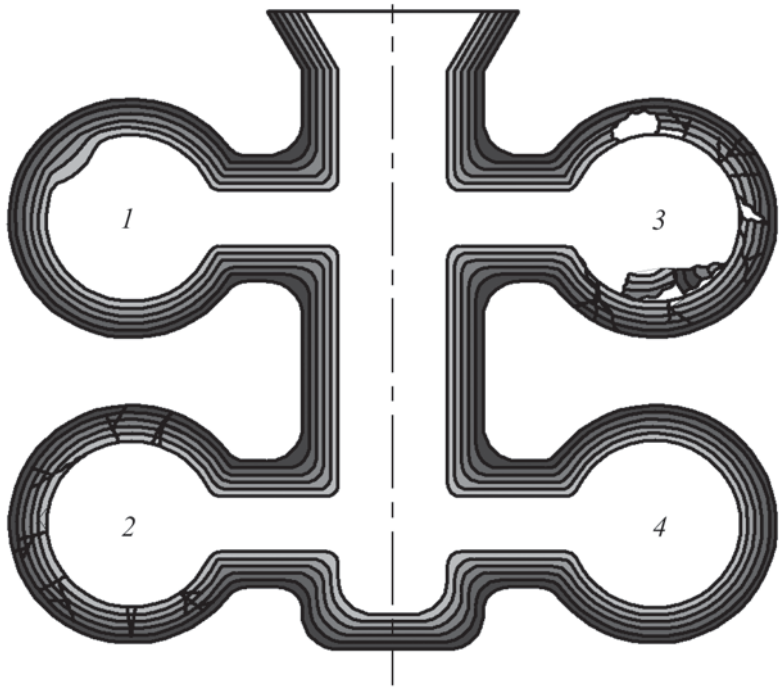

Fig. 1. Investment casting defect formation flowchart for a 5-layer ceramic shell mold

Рис. 1. Схема последовательности появления типичных дефектов, характерных для различных этапов получения отливок методом ЛВМ, на примере 5-слойной керамической оболочковой формы

baking, leading to ceramic fragments getting into the casting;

4 — defect-free ceramic mold cavity.

To mitigate shrinkage-related issues, conventional anti-shrinkage measures include using materials with the required rheological properties or controlling such properties, as well as casting within a narrow temperature range [18; 19].

Casting is a complex and costly process, and any defects are deemed unacceptable, which has prompted the exploration of alternative casting methods.

However, the utilization of new or improved wax materials can result in additional expenses. Most commonly, oil paraffin waxes are employed along with various additives such as stearin, ceresin, rosin, and brown coal wax. One commonly used wax is PS50/50, which is a blend consisting of equal weights of paraffin and stearin [13].

During the solidification of PS50/50 wax, stresses develop within the investment pattern, leading to cracking and chipping. Consequently, enhancing casting accuracy becomes challenging. To address this issue, the preferable approach is to create investment patterns using wax powder due to its superior manufacturability. This method helps reduce stress and allows for improved accuracy, as the powdered material can penetrate even the most intricate cavities [20; 21].

The cold compaction of wax powder in the casting process introduces various factors such as interparticle friction, friction against the mold walls [22], and temperature rise. As the wax grains come into contact, they melt and form a porous matrix that matches the configuration of the mold cavity, thereby preventing shrinkage defects in both the investment pattern and the mold walls.

However, there are drawbacks of this process, including potential geometry distortions when the pressurized air is released and the compacted wax expands. Experimental measurements have shown that the elastic deformation of the wax after the load is removed ranges from 0.7 to 1.2 % in the direction of compression and from 0.4 to 0.5 % in the transverse direction [23]. Compared to liquid or paste-like materials, powder wax cores maintain their dimensions more effectively [24; 25]. While acceptable casting accuracy can be achieved with powder wax patterns, there is still a need to address distortions through experimental studies on the elastic distortion of wax after compaction.

The extent of distortion is influenced by the rheological properties of the wax, including elasticity, plasticity, strength, ductility, and creep. Cold compaction can result in local overheated spots. The magnitude of elastic distortion depends on the stress relaxation time, which is affected by particle size, compaction pressure, and rate. Stress levels increase with greater compaction intensity. The study aimed to determine the point at which the elastic deformation of a compacted material under a constant load becomes irreversible (plastic) [26; 27]. Initial findings revealed that when the compaction (mold closing) rate ranges from 0.25 to 1.5 mm/s, the distortion of powder wax does not exceed 1.2 % in the direction of compaction. The application of forced relaxation by allowing the wax to dwell in the mold under load helps redistribute stress and reduces distortion.

The objective of this study was to compare computational and experimental properties of wax powder to predict dimensional deviations in porous wax patterns relative to the mold cavity dimensions.

The research workflow involved the following steps:

— testing to obtain the stress vs. porosity relationship for powder wax compaction;

— comparison of simulated stress values with actual measurements;

— determination of the factors in the stress relaxation equation for powder wax patterns.

Materials and methods

In order to determine the stress (σ) resulting from variations in strain (ε) over time (τ), we applied the rheological equation:

$$f(\sigma,\varepsilon,\tau) = 0. \quad (1)$$

For the compaction tests of the powder wax, a constant compressive strain (ε = const) was maintained [28]. During the compaction process, the local temperature rises and reaches the melting point. As the load is removed, the temperature decreases. The stress relaxation (σ) in the solidification region of the wax for a constant strain (ε = const) is described by the Kohlrausch equation [29; 30]:

$$\sigma = \sigma_0 \exp^{-(t/a)^b}, \quad (2)$$

where a and b ($0 < b \leq 1$) are constants at a given tempe-

rature and pressure, σ represents the stress at time t; σ_0 is the relaxing component of the stress.

We estimated the factors of the Kohlrausch equation that describe the relaxation properties of the compacted wax using the experimental curves presented by Pavlov V. et al. [31]. For a porous body, the analytical expression for the relaxation curve is

$$\sigma = \sigma_0(P)\exp^{-(t/\tau)^k}, \quad (3)$$

where $\sigma_0(P)$ represents the peak stress at the compaction puncheon when unloading begins for the given porosity P.

The values τ and k in the analytical equation of the relaxation of the porous body are determined using the least squares method. To do this, we denote the measured stress $\tilde{\sigma}_i$ at the moment t_i and express it in terms of $\sigma_0(P)$:$\tilde{\sigma}_i = \sigma(t_i)/\sigma_0(P)$. Finding the parameters of expression (3) involves minimizing the generalized scattering index. We applied the method of least squares not to the original exponential function (2), but to its transformed version (3). Since the values $\tilde{\sigma}_i$ fall within the range $0 < \tilde{\sigma}_i \le 1$, then $\ln\tilde{\sigma}_i \le 0$, and therefore the scattering index can be represented as

$$Q = \sum_{i=1}^{n}\left\{\ln(-\ln\tilde{\sigma}_i) - \ln\left[-\ln(\exp^{-(t_i/\tau)^k})\right]\right\}^2 = \sum_{i=1}^{n}\left[\ln(-\ln\tilde{\sigma}_i) - k\ln(t_i/\tau)\right]^2. \quad (4)$$

When selecting the experimental points, it is importante to consider that when unloading begins at $\tilde{\sigma}_i = 1$ or at $t = 0$, expression (4) does not yet exist. However, we can observe that $\exp^{-(t/\tau)^k}\big|_{t=0} = \tilde{\sigma}_i(t_0) = 1$. We equated the partial derivatives of Q with respect to τ and k to zero:

$$\left.\begin{aligned}\frac{\partial Q}{\partial\tau} &= 2\sum_{i=1}^{n}\left[\ln(-\ln\tilde{\sigma}_i) - k\ln(t_i/\tau)\right]\frac{k}{\tau} = 0,\\ \frac{\partial Q}{\partial\tau} &= -2\sum_{i=1}^{n}\left[\ln(-\ln\tilde{\sigma}_i) - k\ln(t_i/\tau)\right]\ln(t_i/\tau) = 0.\end{aligned}\right\} \quad (5)$$

By transforming system (5), we obtained the normal equations in their standard form:

$$\left.\begin{aligned}kn\ln\left(\frac{1}{\tau}\right) + k\sum_{i=1}^{n}\ln t_i &= \sum_{i=1}^{n}\ln(-\ln\tilde{\sigma}_i),\\ k\ln\left(\frac{1}{\tau}\right)\sum_{i=1}^{n}\ln t_i + k\sum_{i=1}^{n}(\ln t_i)^2 &= \sum_{i=1}^{n}\ln(-\ln\tilde{\sigma}_i)\ln t_i.\end{aligned}\right\} \quad (6)$$

The solution to system (6) is

$$k\ln\left(\frac{1}{\tau}\right) = \frac{\sum_{i=1}^{n}\ln(-\ln\tilde{\sigma}_i)\sum_{i=1}^{n}(\ln t_i)^2 - \sum_{i=1}^{n}\ln(-\ln\tilde{\sigma}_i)\ln t_i\sum_{i=1}^{n}\ln t_i}{n\sum_{i=1}^{n}(\ln t_i)^2 - \left(\sum_{i=1}^{n}\ln t_i\right)^2},$$

$$k = \frac{n\sum_{i=1}^{n}\ln(-\ln\tilde{\sigma}_i)\ln t_i - \sum_{i=1}^{n}\ln(-\ln\tilde{\sigma}_i)\sum_{i=1}^{n}\ln t_i}{n\sum_{i=1}^{n}(\ln t_i)^2 - \left(\sum_{i=1}^{n}\ln t_i\right)^2}. \quad (7)$$

τ is expressed as

$$\tau = \exp\left[\frac{\sum_{i=1}^{n}\ln(-\ln\tilde{\sigma}_i)\ln t_i\sum_{i=1}^{n}\ln t_i - \sum_{i=1}^{n}\ln(-\ln\tilde{\sigma}_i)\sum_{i=1}^{n}(\ln t_i)^2}{n\sum_{i=1}^{n}\ln(-\ln\tilde{\sigma}_i)\ln t_i - \sum_{i=1}^{n}\ln(-\ln\tilde{\sigma}_i)\sum_{i=1}^{n}\ln t_i}\right]. \quad (8)$$

The k and τ parameters of the Kohlrausch equation (3) were determined through experimental analysis using equations (7) and (8).

For wax testing, we utilixed purified paraffin, specifically T1 grade, as well as a 1 : 1 mixture of paraffin and stearin (PS50/50). These materials, classified as Category 1 [13], are commonly employed in investment casting. As the actual properties of the wax may deviate from specified values (e.g., Solid Petroleum Paraffins. Specifications. GOST 23683-89), we measured the density (ρ) and Young's modulus (E): for T1, ρ = 0.86 g/cm^3, E = 81.91 MPa; for PS50/50, ρ = = 0.935 g/cm^3, E = 71.8 MPa. The melting points of T1 and PS50/50 waxes were determined using a Shimadzu DTG-60H differential thermal analyzer, employing a heating rate of 2 °C/min. The melting points were found to be 58 °C and 52 °C, respectively. Due to the relatively low melting points, we conducted the tests within a narrow ambient temperature range of 20±2 °C to enhance accuracy.

The mold used in the experiments was constructed from steel grade 45 (equivalent to US analog: SA-29 1044). Its cavity took the form of a cylindrical shape with an inner diameter of d = 43.3 mm. The mold was assumed to be rigid and non-deformable. The wax patterns were created using T1 and PS50/50 materials with particle sizes of 0.63 mm and 2.5 mm, selected to optimize manufacturability. The bulk den-

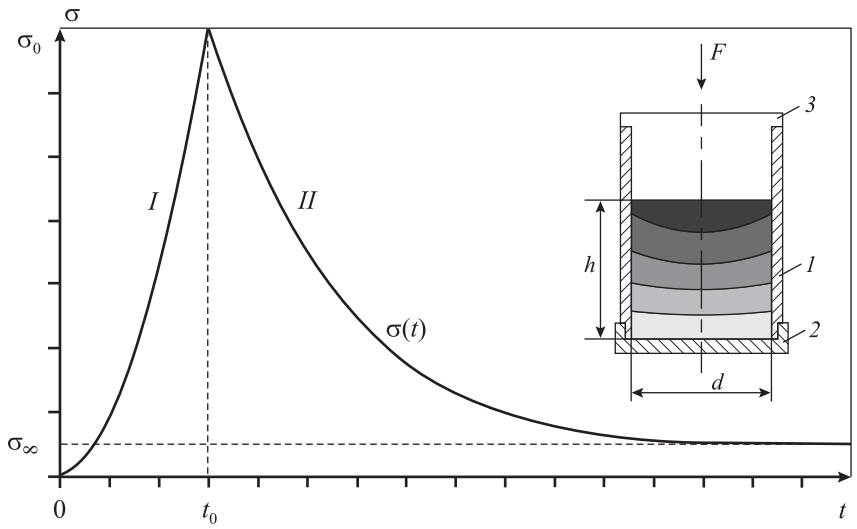

Fig. 2. Loading and relaxation of T1 and PS50 wax powders
I – loading curve, ***II*** – relaxation curve
1 – mold, ***2*** – bottom, ***3*** – puncheon

Рис. 2. Схема нагружения и релаксации порошкового тела из воскообразных материалов Т1 и ПС50/50
I – кривая нагружения, ***II*** – кривая релаксации
1 – пресс-матрица, ***2*** – основание, ***3*** – пресс-пуансон

sity (ρ_{bulk}, g/cm^3) values were as follows: 0.360 (T1, 2.5 mm particle size); 0.320 (T1, 0.63 mm particle size); 0.340 (PS50/50, 2.5 mm particle size); 0.310 (PS50/50, 0,63 mm particle size). The powder was obtained by sieving through 026 sieves, resulting in flake-shaped particles. Consequently, the existing methods used for estimating the final properties of compacted powders with spherical particles [32] were not applicable in this case.

The porosity P of the compacted powders varied within the range of 0 % ≤ P ≤ 12 %, with increments of 2 %. To control the porosity, we manipulated the deformation (ε) of the powder by moving the puncheon at a rate of 1 mm/s untill the same height matched its diameter (h = d, as shown in Fig. 2). Subsequently, we measured the stresses exerted on the sample using an AG-X plus Shimadzu testing machine during a relaxation period of 60 minutes (from t_0 to t_{60}). The maximum load applied was 250 kN. Meeting the machine manufacturer's specifications, a tolerance of 0.03 % was maintained for a load of 100 kN and a deformation of 10 mm, ensuring reliable test results.

Figure 2 illustrates the loading and relaxation process applied to the wax powders during the formation of porous compacted samples using T1 and PS50/50 materials. The porosity of the samples was determined using the following formula

$$P = (1 - \rho_p / \rho_s) \cdot 100\ \%, \qquad (9)$$

where ρ_p represents the density of the porous sample, kg/m^3; ρ_s represents the density of the solid cast sample, kg/m^3.

To determine the appropriate porosity range, we evaluated the mechanical properties of the samples. It was observed that samples with porosity exceeding 12 % exhibited low surface hardness and strength, rendering them unsuitable for use. The wax powder weight (M, kg) required to produce a sample with the desired porosity P was estimated using the following equation:

$$M = h\rho_s \left(1 - \frac{P}{100}\right)\left(\frac{\pi d^2}{4}\right). \qquad (10)$$

In this case, h = d = 0.0433 m. We calculated the necessary weights of T1 and PS50/50 waxes to achieve the specified sample porosity using the following empirical relationships obtained from experimentation:

$$M_{T1} = -0{,}55P + 55,$$

$$M_{PS50/50} = -0{,}5959P + 59.59.$$

Once the height h was reached, the loading arm of the AG-X plus Shimadzu machine remained stationary for a duration of 60 minutes while the stresses were recorded. During this time, as the air within the sample was expelled and the density redistributed, the stresses experienced a reduction but were not always completely eliminated. Consequently, the dimensions of the sample underwent changes due to the elastic reaction of the compacted material, which can be quantified as follows:

$$O = \frac{(d_i - d)}{d_i} \cdot 100\ \%, \qquad (11)$$

where O represents the elastic deformation, %; d and d_i denote the inner diameter of the mold and the height of the i-th samples, respectively. These measurements were obtained using a DIN 863 Vogel digital recorder with an accuracy of 0.001 mm.

Furthermore, the AG-X plus Shimadzu determined the compressive strength of the compacted samples at a loading arm velocity of 0.1 mm/s. This evaluation took place after the samples were held at a controlled temperature of 20±2 °C for a period of 48 hours.

Discussion

Figure 3 displays the experimental findings, illustrating exponential relationships between the stress σ_0 within samples composed of compacted T1 and PS50/50 powder waxes with particle sizes 2.5 mm and 0.63 mm, respectively, and the porosity (as the controllable variable). The figure also demonstrates the reliability of the polynomial approximation $1R^2_{2.5}$; $2R^2_{0.63}$; $3R^2_{2.5}$ и $4R^2_{0.63}$ for these specific samples.

Figure 3 demonstrates that the stresses observed in samples with a particle size of 2.5 mm are higher compared to those with a particle size of 0.63 mm across all materials investigated. This relationship can be attributed to the higher bulk density exhibited by the 2.5 mm samples in comparison to the 0.63 mm samples. Additionally, the compaction stress is influenced by the plasticity of the powder, which, in turn, is influenced by the melting point [33; 34]. Given that the melting point of T1 is higher than that of PS50/50, the stress observed in T1 is greater than in PS50/50. It was observed that when the particle size of the T1 and PS50/50 materials

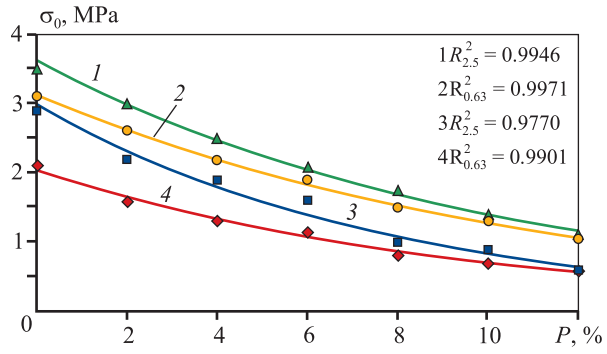

Fig. 3. Stress vs. porosity in the T1 and PS50/50 powder wax samples

1 – T1, 2.5 mm particle size; ***2*** – T1, 0.63 mm particle size; ***3*** – PS50/50, 2.5 mm particle size; ***4*** – PS50/50, 0.63 mm particle size

Рис. 3. Сравнение зависимостей напряжений от пористости прессовок из порошков воскообразных материалов Т1 и ПС50/50 различных фракций

1 – Т1, фракция 2,5 мм; ***2*** – Т1, фракция 0,63 мм; ***3*** – ПС50/50, фракция 2,5 мм; ***4*** – ПС50/50, фракция 0,63 мм

increases four-fold within the range of 0 % ≤ P ≤ 2 %, the difference in stresses reaches 30 %. As P increases, the difference diminishes.

From a practical standpoint, it is valuable to compare the stresses observed in wax patterns with different particle sizes to the breaking stresses of the experimental samples exhibiting the same porosity. Figure 4 illustrates the relationship between the ultimate compressive strength (σ_{comp}) and porosity of the cylindrical samples. It is evident that the breaking stress increases with particle size. It can be concluded that while T1 samples exhibit greater resistance to compression compared to PS50/50 samples, the latter are sufficiently robust to endure the compressive loads applied by the initial (uncured) layer of the refractory shell.

To assess the compressive strength of compacted wax patterns, we introduced the stress safety margin N_{comp}. This margin represents the ratio of the ultimate compressive strength to the stress experienced during the compression of the powder wax. The stress safety margin can be calculated as follows:

$$N_{comp} = (\sigma_{comp} \cdot 100\ \%)/\sigma_0, \qquad (12)$$

where σ_{comp} represents the compressive strength, MPa; aand σ_0 is the compression stress measured by the test machine, MPa.

Figure 5 illustrates the stress safety margin (N_{comp}) as a function of sample porosity within the range of 0 % to 12 % for T1 and PS50/50 waxes, considering particle sizes of 0.63 mm and 2.5 mm.

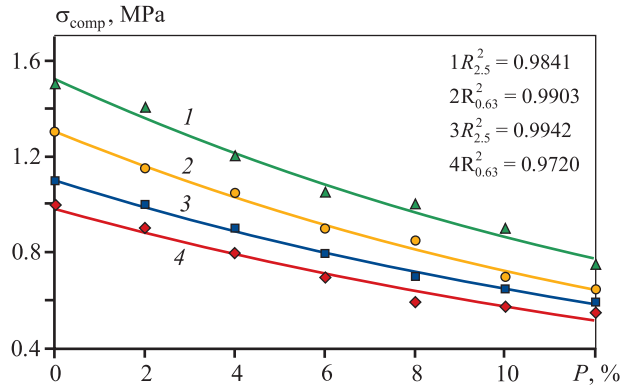

Fig. 4. Ultimate compressive strength vs. porosity in the T1 and PS50/50 powder wax samples

1 – T1, 2.5 mm particle size; ***2*** – T1, 0.63 mm particle size;
3 – PS50/50, 2.5 mm particle size;
4 – PS50/50, 0.63 mm particle size

Рис. 4. Сравнение зависимостей предела прочности на сжатие от пористости прессовок из порошков воскообразных материалов Т1 и ПС50/50 различных фракций

1 – Т1, фракция 2,5 мм; ***2*** – Т1, фракция 0,63 мм;
3 – ПС50/50, фракция 2,5 мм;
4 – ПС50/50, фракция 0,63 мм

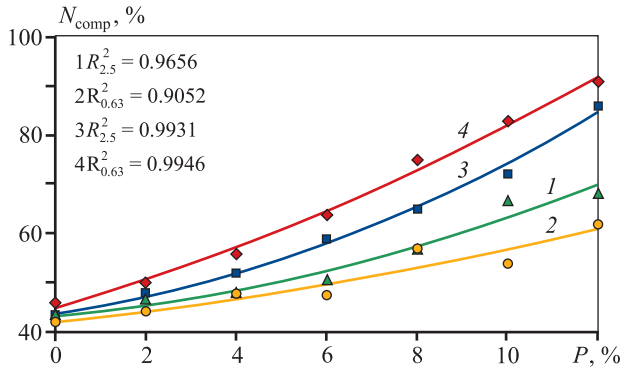

Fig. 5. Stress safety margin vs. porosity of T1 and PS50/50 powder wax samples

1 – T1, 2.5 mm particle size; ***2*** – T1, 0.63 mm particle size;
3 – PS50/50, 2.5 mm particle size;
4 – PS50/50, 0.63 mm particle size

Рис. 5. Сравнение зависимостей показателя пропорциональности напряжений от пористости прессовок из порошков воскообразных материалов Т1 и ПС50/50 различных фракций

1 – Т1, фракция 2,5 мм; ***2*** – Т1, фракция 0,63 мм;
3 – ПС50/50, фракция 2,5 мм;
4 – ПС50/50, фракция 0,63 мм

Using Fig. 5, we can predict the compressive strength of a wax pattern by using the stress safety margin value. For example, if we have a T1 wax sample with a particle size of 0.63 mm and a porosity of 8 %, the ultimate strength σ_{comp} is estimated to be 57 % of the σ_0 stress applied during wax compaction.

Additionally, when measuring the relaxation stresses σ_i in the samples following compression, we observed significant changes in σ_i values within a maximum of 25 minutes for all particle sizes. The time required for σ_i to decrease is longer for samples with a porosity of 2.5 mm compared to those with a particle size of 0.63 mm, particularly in cases of higher porosity. Overall, the relaxation period for PS50/50 wax samples is shorter compared to T1 wax samples. The table presents the experimentally determined values of k and τ for the Kohlrausch equation (obtained from equations (7) and (8)) for samples with 0 % and 12 % porosity. It is noteworthy that k and τ decrease as the porosity increases for all materials. By substituting the values of k and τ into the analytical expression (3), we can obtain the predicted relaxation curves.

Figure 6 displays the estimated and experimental relaxation periods for the T1 (Fig. 6, *a* and *b*) and PS50/50 (Fig. 6, *c* and *d*) samples, considering particle sizes of 2.5 mm and 0.63 mm, respectively.

Figure 6 illustrates that the experimental σ_i stress values, which occur as the compacted material is unloaded, decrease slightly faster than predicted by the exponential law. It was observed that significant changes (more than 90 % reduction) in the experimental σ_i values are achieved within the first 5 minutes and 10 minutes of holding under load for the samples with 12 % and 0 % porosity, respectively. This pattern holds true for all wax grades and particle sizes. Generally, the trends of the estimated and experimental σ_i values align closely with each other.

Conclusion

The study revealed several key findings regarding the compaction and behavior of wax patterns. Firstly, it was observed that the stresses measured during the compaction of larger 2.5 mm particle size powder samples were higher than those of the 0.63 mm particle size samples for all materials. This discrepancy can be attributed to the higher bulk density of the 2.5 mm particle size wax compared to the 0.63 mm particle size wax, as well as differences in the elastic properties and melting points.

Experimental *k* and τ values for the Kohlrausch equation

Расчетные параметры *k* и τ для уравнения Кольрауша, определенные по экспериментальным данным

Wax grade	Particle size, mm	Porosity,%	Analytical expression variables	
			k	τ
T1	2.5	0	0.729	3.034
	2.5	12	0.589	1.478
	0.63	0	0.568	2.058
	0.63	12	0.375	0.706
PS50/50	2.5	0	0.722	3.250
	2.5	12	0.401	1.023
	0.63	0	0.566	2.453
	0.63	12	0.313	0.742

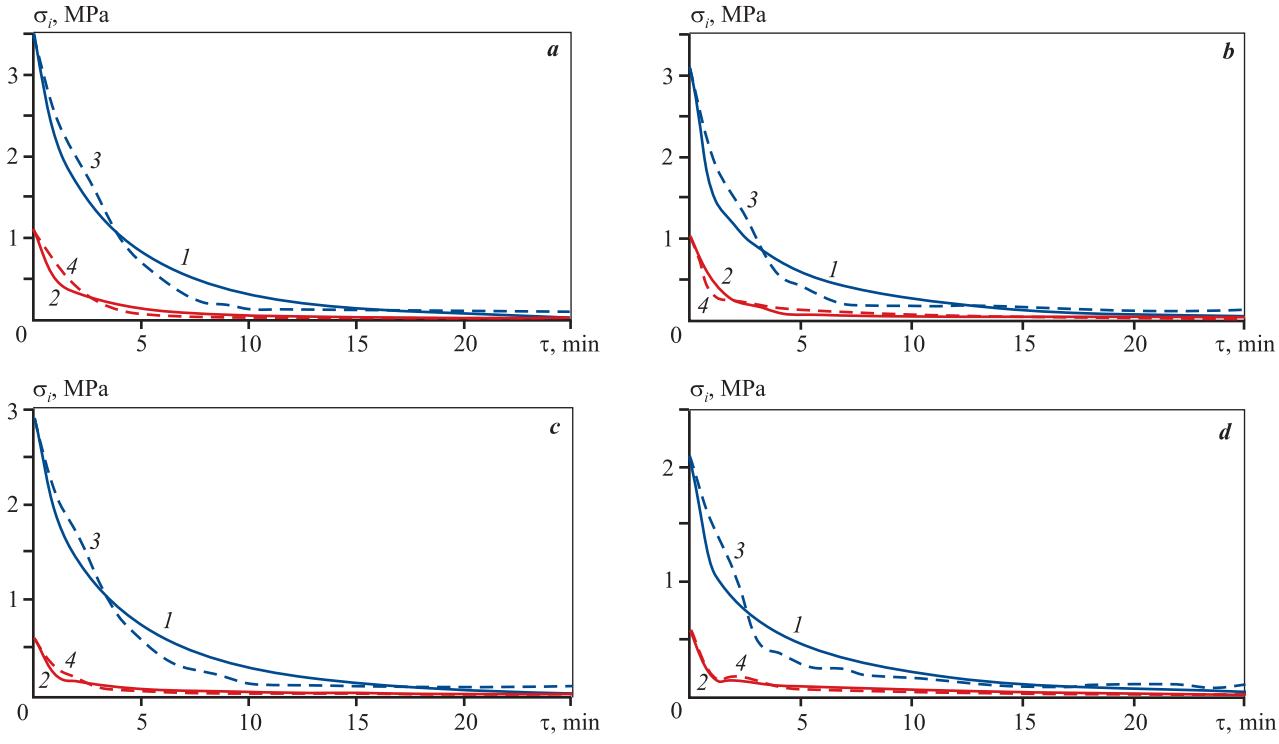

Fig. 6. Experimental and estimated stress vs. relaxation period curves for different wax grades and particle sizes

a – T1, 2.5 mm particle size; ***b*** – T1, 0.63 mm particle size; ***c*** – PS50/50, 2.5 mm particle size; ***d*** – PS50/50, 0.63 mm particle size
1, ***3*** – $P = 0$ %; 2, 4: $P = 12$ %
Solid curves – estimated, dashed curves – experimental

Рис. 6. Сравнение экспериментальных и расчетных экспоненциальных зависимостей напряжений от времени релаксации прессовок для различных материалов и фракций

a – T1, фракция 2,5 мм; ***b*** – T1, фракция 0,63 мм; ***c*** – ПС50/50, фракция 2,5 мм; ***d*** – ПС50/50, фракция 0,63 мм
1, ***3*** – $P = 0$ %; ***2***, ***4*** – $P = 12$ %
Сплошные кривые – расчет, штриховые – эксперимент

Additionally, the compressive breaking stress was found to be dependent on both sample porosity and particle size. The proposed stress safety margin provides a means to predict the compression strength of compacted wax patterns.

By utilizing the Kohlrausch equation, exponential relationships were established to describe the stress decrease over time. It was noted that the measured σ_i stresses occurring as the compacted wax is unloaded exhibited a slightly faster decrease than predicted by the exponential law. Significant changes in σ_i were mostly completed within the first 5 to 10 minutes of holding under load. A zero stress reading after relaxation indicated the absence of elastic deformation and confirmed the preservation of the required sample dimensions.

The research outcomes have practical implications for predicting the final dimensions of compacted powder wax patterns and enhancing the accuracy of investment casting. The proposed casting process involves the utilization of wax powder with particle sizes ranging from 0.63 mm to 2.5 mm, replacing the use of liquid or paste wax. The wax patterns are compressed and subsequently held under load. The resulting wax patterns exhibited improved quality, with no defects such as shrinkage, surface waviness, or buckling. The porosity of the samples was evenly distributed, reducing mold shell deformation during wax removal and enhancing the resistance to cracking, ultimately leading to improved casting quality.

References

1. Dogancan Okumus, Sefer A. Gunbeyaz, Rafet Emek Kurt, Osman Turan. Towards a circular maritime industry: Identifying strategy and technology solutions. *Journal of Cleaner Production*. 2023;382:134935. https://doi.org/10.1016/j.jclepro.2022.134935
2. Gogolukhina M., Mamedova L. Organisational and economic aspects of deep modernisation and foundation projects of shipbuilding yards. *Transportation Research Procedia*. 2022;63:2072—2078. https://doi.org/10.1016/j.trpro.2022.06.231
3. Chernyshov E.A., Romanov A.D., Romanova E.A. The quality control of high-resistance steel casting by optimizing the tempering temperature. *Materials Today: Proceedings*. 2021;38(4):1488—1490. https://doi.org/10.1016/j.matpr.2020.08.134
4. Abayomi A. Akinwande, Adeolu A. Adediran, Oluwatosin A. Balogun, Moses Ebiowei Yibowei, Abel A. Barnabas, Henry K. Talabi, Bayode J. Olorunfemi. Optimization of selected casting parameters on the mechanical behaviour of Al 6061/glass powder composites. *Heliyon*. 2022;8(5):e09350. https://doi.org/10.1016/j.heliyon.2022.e09350
5. Li Changyun, Wu Shiping, Guo Jingjie, Su Yanqing, Bi Weisheng, Fu Hengzhi. Model experiment of mold filling process in vertical centrifugal casting. *Journal of Materials Processing Technology*. 2006;176(1—3):268—272. https://doi.org/10.1016/j.jmatprotec.2006.04.004
6. Yiping Lu, Xuzhou Gao, Li Jiang, Zongning Chen, Tongmin Wang, Jinchuan Jie, Huijun Kang, Yubo Zhang, Sheng Guo, Haihui Ruan, Yonghao Zhao, Zhiqiang Cao, Tingju Li. Directly cast bulk eutectic and near-eutectic high entropy alloys with balanced strength and ductility in a wide temperature range. *Acta Materialia*. 2017;124:143—150. https://doi.org/10.1016/j.actamat.2016.11.016
7. Krushenko G.G. Improvement of quality of steel casted propeller for river passenger vessel. *Sudostroenie*. 2016;6(829):54—57. (In Russ).
Крушенко Г.Г. Повышение качества стального литого гребного винта для пассажирского речного судна. *Судостроение*. 2016;6(829):54—57.
8. Markov S.P., Muktepavel V.O., Murzin V.V. Surface hardening of the bronze ship propeller. *Morskie intellektual'nye tekhnologii*. 2019;4-1(46):97—101. (In Russ.).
Марков С.П., Муктепавел В.О., Мурзин В.В. Поверхностное упрочнение судовых гребных винтов из бронзы. *Морские интеллектуальные технологии*. 2019;4-1(46):97—101.
9. Abashkin E.E., Tkacheva A.V. Study of local combined heat impact on permanent joints. *Morskie intellektual'nye tekhnologii*. 2022;3-1(57):310—318. (In Russ.). https://doi.org/10.37220/MIT.2022.57.3.040
Абашкин Е.Е., Ткачева А.В. Влияние предварительного подогрева пластины на значения и распределение остаточных напряжений, образованных в результате наплавки. *Морские интеллектуальные технологии*. 2022;3-1(57):310—318. https://doi.org/10.37220/MIT.2022.57.3.040
10. Ayar M.S., Ayar V.S., George P.M. Simulation and experimental validation for defect reduction in geometry varied aluminium plates casted using sand casting. *Materials Today: Proceedings*. 2020;27:1422—1430. https://doi.org/10.1016/j.matpr.2020.02.788

11. Pan Tao, Heng Shao, Zhijun Ji, Hai Nan, Qingyan Xu. Numerical simulation for the investment casting process of a large-size titanium alloy thin-wall casing. *Progress in Natural Science: Materials International.* 2018;28(4): 520—528. https://doi.org/10.1016/j.pnsc.2018.06.005
12. Kapranos P., Carney C., Pola A., Jolly M. 5.03 — Advanced casting methodologies: Investment casting, centrifugal casting, squeeze casting, metal spinning, and batch casting. *Comprehensive Materials Processing.* 2014;5:39—67. https://doi.org/10.1016/B978-0-08-096532-1.00539-2
13. Garanin V.F., Ivanov V.N., Kazennov S.A., Kurchman B.S., Lishchenko N.N., Ozerov V.A., Roshan N.R., Sokol I.B., Telis M.Ya., Chulkova A.D., Shklennik Ya.I., Shklennik L.Ya. Investment casting. Ed. V.A. Ozerov. 4th ed. Moscow: Mashinostroenie, 1994. 448 p. (In Russ.).
Гаранин В.Ф., Иванов В.Н., Казеннов С.А., Курчман Б.С., Лищенко Н.Н., Озеров В.А., Рошан Н.Р., Сокол И.Б., Телис М.Я., Чулкова А.Д., Шкленник Я.И., Шкленник Л.Я. Литье по выплавляемым моделям. Под общ. ред. В.А. Озерова. 4-е изд., перераб. и доп. М.: Машиностроение, 1994. 448 с.
14. Radtsevich Kh.M. Calculation of allowances and interoperational dimensions in mechanical engineering: textbook. allowance. Moscow: Vysshaya shkola, 2004. 272 p. (In Russ.).
Радцевич Х.М. Расчет припусков и межоперационных размеров в машиностроении: Учеб. пос. М.: Высшая школа, 2004. 272 с.
15. Prokopchuk N.R., Gorshcharik N.D., Klyuev A.Yu., Kozlov N.G., Rozhkova E.I., Latyshevich I.A., Bakovich N.A. Model compositions for precision casting. *Vestsi Natsyyanal'nai akademii navuk Belarusi. Seryya khimichnykh navuk*. 2015;(4): 122—128. (In Russ.).
Прокопчук Н.Р., Горщарик Н.Д., Клюев А.Ю., Козлов Н.Г., Рожкова Е.И., Латышевич И.А., Бакович Н.А. Модельные составы для точного литья. *Весці Нацыянальнай акадэміі навук Беларусі. Серыя хімічных навук*. 2015;(4):122—128.
16. Sapchenko I.G., Zhilin S.G., Komarov O.N. Controlling the structure and properties of porous combined removable models. Vladivostok: Dal'nauka, 2007. 138 p. (In Russ.).
Сапченко И.Г., Жилин С.Г., Комаров О.Н. Управление структурой и свойствами пористых комбинированных удаляемых моделей. Владивосток, Дальнаука, 2007. 138 с.
17. Foggia M.Di, D'Addona D.M. Identification of critical key parameters and their impact to zero-defect manufacturing in the investment casting process. *Procedia CIRP.* 2013;12:264—269. https://doi.org/10.1016/j.procir.2013.09.046
18. Ospennikova O.G. Thermophysical and rheological characteristics of synthetic resins for model compositions. *Liteinoe Proizvodstvo*. 2016;(10):26—28. (In Russ.).
Оспенникова О.Г. Теплофизические и реологические характеристики синтетических смол для модельных композиций. *Литейное производство.* 2016;(10):26—28.
19. Tascioglu S., Akar N. Conversion of an investment casting sprue wax to a pattern wax by chemical agents. *Materials and Manufacturing Processes.* 2003; 18(5):753—768. https://doi.org/10.1081/AMP-120024973
20. Sapchenko I.G., Zhilin S.G., Potianikhin D.A., Komarov O.N. Mesomechanics of technological properties of powdered polymer compacts in Lost Wax Casting. *AIP Conference Proceedings.* 2014;1623:543—546. https://doi.org/10.1063/1.4899002
21. Vinokurov G.G., Popov O.N. Statistical modeling of local density macrostructure correlation at one-sided pressing of powder materials. *Izvestiya Samarskogo nauchnogo tsentra RAN.* 2011;13(1—3)(39):553—557. (In Russ.).
Винокуров Г.Г., Попов О.Н. Статистическое моделирование корреляции локальной плотности макроструктуры при одностороннем прессовании порошковых материалов. *Известия Самарского научного центра РАН.* 2011;13(1—3)(39):553—557.
22. Zhilin S.G., Komarov O.N., Bogdanova N.A., Amosov O.S. Mathematical modelling of forming processes in the conditions of uniaxial compaction of powder wax-like materials. In: *CEUR Workshop Proceedings. "ITHPC 2021 — Short paper proceedings of the 6th International Conference on information technologies and high-performance computing"*. 2021. P. 148—154.
23. Zhilin S.G., Bogdanova N.A., Komarov O.N., Sosnin A.A. Decrease in the elastic response in compacting a paraffin—stearin powder composition. *Russian Metallurgy (Metally).* 2021;(4):459—463. https://doi.org/10.1134/S0036029521040376
Жилин С.Г., Богданова Н.А., Комаров О.Н., Соснин А.А. Снижение упругого отклика при уплотнении порошковой парафиностеариновой композиции. *Деформация и разрушение материалов.* 2020;(1):29—33. https://doi.org/10.31044/1814-4632-2020-1-29-33

24. Dong Y.W., Li X.L., Qi Zhao, Jun Yang, Ming Dao. Modeling of shrinkage during investment casting of thin-walled hollow turbine blades. *Journal of Materials Processing Technology*. 2017;244:190—203. https://doi.org/10.1016/j.jmatprotec.2017.01.005
25. Michio Ito, Toshio Yamagishi, Yoshiki Oshida, Carlos A. Munoz. Effect of selected physical properties of waxes on investments and casting shrinkage. *The Journal of Prosthetic Dentistry*. 1996;75(2):211—216. https://doi.org/10.1016/S0022-3913(96)90101-8
26. Malkin A.Ya., Isaev A.I. Rheology. Concepts, methods, applications. Moscow: Professiya, 2007. 560 p. (In Russ.).
Малкин А.Я., Исаев А.И. Реология. Концепции, методы, приложения. М.: Профессия, 2007. 560 с.
27. Malkin A.Ya., Chalykh A.E. Diffusion and viscosity of polymers. Moscow: Khimiya, 1979. 304 p. (In Russ.).
Малкин А.Я., Чалых А.Е. Диффузия и вязкость полимеров. М.: Химия, 1979. 304 с.
28. Galperin A.M., Shafarenko E.M., Rheological calculations of mining structures. Moscow: Nedra, 1977. 246 p. (In Russ.).
Гальперин А.М., Шафаренко Е.М. Реологические расчеты горнотехнических сооружений. М.: Недра, 1977. 246 с.
29. Zhilin S.G., Komarov O.N., Potyanikhin D.A., Sosnin A.A. Experimental determining parameters of Kohlrausch regression dependence for porous compacts from waxy powder compositions. *Inzhenernyi zhurnal: Nauka i innovatsii*. 2018;2(74):9. (In Russ.). http://doi.org/10.18698/2308-6033-2018-2-1732
Жилин С.Г., Комаров О.Н., Потянихин Д.А., Соснин А.А. Экспериментальное определение параметров регрессионной зависимости Кольрауша для пористых прессовок из воскообразных порошковых композиций. *Инженерный журнал: Наука и инновации*. 2018;2(74):9. http://doi.org/10.18698/2308-6033-2018-2-1732
30. Zhilin S.G., Bogdanova N.A., Komarov O.N. Influence of parameters of the compacting of powder body from wax-like material on the forming of residual stresses of pressing. *Vestnik Chuvashskogo gosudarstvennogo pedagogicheskogo universiteta im. I.Ya. Yakovleva. Seriya: Mekhanika predel'nogo sostoyaniya*. 2019;3(41):110—121. (In Russ.). http://doi.org/10.26293/chgpu.2019.41.3.009
Жилин С.Г., Богданова Н.А., Комаров О.Н. Влияние параметров уплотнения порошкового тела из воскообразного материала на формирование остаточных напряжений прессовки. *Вестник Чувашского государственного педагогического университета им. И.Я. Яковлева. Серия: Механика предельного состояния*. 2019;3(41):110—121. http://doi.org/10.26293/chgpu.2019.41.3.009
31. Pavlov V.I., Askadskii A.A., Slonimskii G.L. Graph-analytical method for calculating the mechanical characteristics of a material by stress relaxation at constant deformation. *Mekhanika polimerov*. 1965;(6):16—19. (In Russ.).
Павлов В.И., Аскадский А.А., Слонимский Г.Л. Графоаналитический способ расчета механических характеристик материала по реакции напряжения при постоянной деформации. *Механика полимеров*. 1965;(6):16—19.
32. Pribytkov G.A., Korzhova V.V., Korosteleva E.N. Strength properties and features of destruction of composites of Al—Cr and Al—Cr—Si systems obtained by hot compaction of powder mixtures. *Deformatsiya i razrushenie materialov*. 2013;(8):13—20. (In Russ.).
Прибытков Г.А., Коржова В.В., Коростелева Е.Н. Прочностные свойства и особенности разрушения композитов систем Al—Cr и Al—Cr—Si, полученных горячим уплотнением порошковых смесей. *Деформация и разрушение материалов*. 2013;(8):13—20.
33. Nicole K. Aragon, Sheng Yin, Hojun Lim, Ill Ryu. Temperature dependent plasticity in BCC micropillars. *Materialia*. 2021;19:101181. https://doi.org/10.1016/j.mtla.2021.101181
34. Remo N. Widmer, Alexander Groetsch, Guillaume Kermouche, Ana Diaz, Gilles Pillonel, Manish Jain, Rajaprakash Ramachandramoorthy, Laszlo Pethö, Jakob Schwiedrzik, Johann Michler. Temperature-dependent dynamic plasticity of micro-scale fused silica. *Materials & Design*. 2022;215:110503. https://doi.org/10.1016/j.matdes.2022.110503

Information about the authors

Sergey G. Zhilin — Cand. Sci. (Eng.), Associate Prof., Leading Researcher, Laboratory for the Problems of Creation and Processing of Materials and Products, Institute of Machinery and Metallurgy of Far-Eastern Branch of the Russian Academy of Sciences.
https://orcid.org/0000-0002-0865-7109
E-mail: sergeyzhilin1@rambler.ru

Nina A. Bogdanova — Junior Researcher, Laboratory of Problems of Creation and Processing of Materials and Products, Institute of Machinery and Metallurgy of Far Eastern Branch of the Russian Academy of Sciences.
https://orcid.org/0000-0002-8769-8194
E-mail: joyful289@inbox.ru

Oleg N. Komarov — Cand. Sci. (Eng.), Associate Prof., Director of Institute of Machinery and Metallurgy of Far-Eastern Branch of the Russian Academy of Sciences.
https://orcid.org/0000-0002-7121-4271
E-mail: olegnikolaevitsch@rambler.ru

Информация об авторах

Сергей Геннадьевич Жилин — к.т.н., доцент, вед. науч. сотрудник лаборатории проблем создания и обработки материалов и изделий Института машиноведения и металлургии (ИМиМ) ДВО РАН.
https://orcid.org/0000-0002-0865-7109
E-mail: sergeyzhilin1@rambler.ru

Нина Анатольевна Богданова — мл. науч. сотрудник лаборатории проблем создания и обработки материалов и изделий ИМиМ ДВО РАН.
https://orcid.org/0000-0002-8769-8194
E-mail: joyful289@inbox.ru

Олег Николаевич Комаров — к.т.н., доцент, директор ИМиМ ДВО РАН.
https://orcid.org/0000-0002-7121-4271
E-mail: olegnikolaevitsch@rambler.ru

Contribution of the authors

Sergey G. Zhilin — determination of the purpose of the work, participation in the processing of experimental data and discussion of the results, writing the article.

Nina A. Bogdanova — conducting experiments, participation in the processing of experimental data and discussion of the results.

Oleg N. Komarov — participation in the processing of experimental data and discussion of the results.

Вклад авторов

С.Г. Жилин — определение цели работы, участие в обработке экспериментальных данных и обсуждении результатов, написание статьи.

Н.А. Богданова — проведение экспериментов, участие в обработке экспериментальных данных и обсуждении результатов.

О.Н. Комаров — участие в обработке экспериментальных данных и обсуждении результатов.

The article was submitted 23.03.2023, revised 06.04.2023, accepted for publication 10.04.2023

Статья поступила в редакцию 23.03.2023, доработана 06.04.2023, подписана в печать 10.04.2023